

Revealing of hidden quantum steerability using local filtering operations

Tanumoy Pramanik,^{1,*} Young-Wook Cho,¹ Sang-Wook Han,¹ Sang-Yun Lee,¹ Yong-Su Kim,^{1,2,†} and Sung Moon^{1,2}

¹*Center for Quantum Information, Korea Institute of Science and Technology (KIST), Seoul, 02792, Republic of Korea*

²*Division of Nano & Information Technology, KIST School,*

Korea University of Science and Technology, Seoul 02792, Republic of Korea

(Dated: December 14, 2024)

Nonlocal quantum correlation is at the heart of bizarre nature of quantum physics. While there are various classes of nonlocal quantum correlation, steerability of a quantum state by local measurements provides unique operational features. Here, we theoretically and experimentally investigate the ‘hidden’ quantum steerability. In particular, we find that there are initially unsteerable states which can reveal the steerability by using local filters on individual quantum systems. It is remarkable that a certain set of local filters are more effective on revealing steerability than Bell nonlocality whereas there exists another set of filters that is more effective on revealing Bell nonlocality than steerability. Finally, we present a counter-intuitive result that mixed states originating from non-maximally pure entangled states can have hidden steerability while the mixed state from a maximally pure entangled state fails to show steerability.

I. INTRODUCTION

Since Einstein, Podolsky and Rosen suggested the EPR paradox, nonlocal quantum correlation has been understood as one of the most peculiar nature of quantum physics [1]. While entanglement has attracted a lot of attention, it has been known that there are other classes of nonlocal quantum correlation such as Bell nonlocality and quantum steerability. [2–5]. Among them, steerability of quantum states by local measurements, which was first suggested by Schrödinger [6], provides unique operational features of quantum theory.

Although the concept of quantum steerability has been recognized from the early stage of quantum physics, its definition and mathematical description have been recently introduced [3, 4]. The operational meaning of quantum steerability can be understood as follows. Let us assume that Alice prepares two systems A and B in an entangled state and sends the system B to Bob. Bob agrees that the prepared state is steerable if Alice can control the state of system B with only local measurements on her system A , and the degree of controllability cannot be explained by local hidden state (LHS) model.

This interpretation leads a remarkable consequence that verification of quantum steerability can be considered as verification of entanglement with an untrusted party (here, Alice), and thus, all the steerable states are entangled. However, it is notable that not all the entangled states guarantee steerability [3, 4]. On the other hand, Bell nonlocality, another nonlocal quantum correlation determined by local hidden variable (LHV) model, guarantees the steerability, while the reverse is not true [7]. Therefore, quantum steerability lies between entanglement and Bell nonlocality.

Besides the entanglement verification, quantum steerability can be a resource for secure quantum communica-

tion when one of the systems (here, the system A) is not trusted as a quantum system. This scenario is known as one-sided device independent quantum key distribution (1s DI-QKD) [8]. Similarly, Bell nonlocality guarantees the security of quantum key distribution in fully device independent manner known as DI-QKD [9–12]. Note that the implementation of 1s DI-QKD is more practical than that of DI-QKD since quantum steerability is more robust against environmental noise and losses than Bell nonlocality [13–15].

The characterization and quantification of quantum steerability are, therefore, of great importance not only for fundamental quantum information science but also for applications in quantum communication. Due to difficulty in finding LHS model for mixed entangled states, however, characterizing steerability is not a simple task. It becomes even more complicated since there are unsteerable states that become steerable when local measurements are performed on multiple copies of the pairs rather than a single copy [16]. Note that this phenomenon is called super-activation of quantum steerability, and a similar phenomenon can also be found in Bell nonlocality [17–19].

In this paper, motivated by hidden Bell nonlocality [20–25], we theoretically and experimentally investigate the revealing of ‘hidden’ quantum steerability by using local filters. In particular, we present that there exist bipartite states, which are initially *not* steerable, can become steerable with the help of local filtering operations on the individual systems. Remarkably, we found that there exists a certain set of local filters that is more effective on revealing steerability than Bell nonlocality while there are another set of filters which is more effective on revealing Bell nonlocality than steerability. We also present a counter-intuitive result that mixed states which are obtained from non-maximally pure entangled states can show hidden steerability for more wide range of a mixing parameter than the mixed state originated from a maximally pure entangled state.

* tanu.pra99@gmail.com

† yong-su.kim@kist.re.kr

II. THEORY

A. Quantum steerability

Let us first briefly introduce the mathematical descriptions of quantum steerability [3, 4]. According to the LHS model, the correlation $P(a_{\mathcal{A}}, b_{\mathcal{B}})$ between the measurement outcomes a and b of the observables \mathcal{A} and \mathcal{B} on the systems A and B can be written as

$$P(a_{\mathcal{A}}, b_{\mathcal{B}}) = \sum_{\lambda} P(\lambda) P(a_{\mathcal{A}}|\lambda) P_Q(b_{\mathcal{B}}|\lambda), \quad (1)$$

where $P(\lambda)$ is the distribution of hidden variables. The subscript Q presents that Bob's probability distribution is obtained from the measurement of observable on the quantum system B . Therefore, a bipartite state ρ shared by Alice and Bob is said to be steerable from Alice to Bob if there exist measurement strategies for Alice and Bob for which the joint probability distribution $P_{\rho}(a_{\mathcal{A}}, b_{\mathcal{B}})$ given by

$$P_{\rho}(a_{\mathcal{A}}, b_{\mathcal{B}}) = \text{Tr} \left[\left(\frac{I + (-1)^a \mathcal{A}}{2} \otimes \frac{I + (-1)^b \mathcal{B}}{2} \right) \rho \right] \quad (2)$$

cannot be explained by the LHS model of Eq. (1).

Experimentally testable steering criteria can be derived from the operational definition of steering. According to the operational definition, if Alice can control the state of Bob's system, then Alice can project the state of Bob's system in the eigenstate of an observable chosen from the set of two non-commuting observables with the precision higher than the predicted value by uncertainty principle. Several steering criteria have been derived based on different forms of uncertainty relation along with the LHS model [26–32].

In order to check the steerability of ρ , we use the fine-grained steering criterion [28]. Note that while the fine-grained steering criterion utilizes two observables for each system, it provides the same steerable-unsteerable boundary with that of the criterion with infinite number of observables. According to the fine-grained steering criterion, the state ρ is steerable (from Alice to Bob) if the conditional probability distribution $P(b_{\mathcal{B}}|a_{\mathcal{A}})$ violates the inequality of

$$T = \frac{1}{2} [P(b_{\mathcal{B}_1}|a_{\mathcal{A}_1}) + P(b_{\mathcal{B}_2}|a_{\mathcal{A}_2})] \leq \frac{3}{4}. \quad (3)$$

Here, $\mathcal{A}_{1,2}$ and $\mathcal{B}_{1,2}$ are non-commuting observables chosen by Alice and Bob, respectively.

B. Hidden quantum correlation

In order to investigate hidden quantum correlation, let us assume that Alice and Bob share a bipartite state of

$$\rho = p |\psi_{\theta}\rangle\langle\psi_{\theta}| + (1-p) \rho_A \otimes \frac{I}{2}, \quad (4)$$

where $|\psi_{\theta}\rangle = \cos\theta |00\rangle + \sin\theta |11\rangle$, $\rho_A = \text{Tr}_B [|\psi_{\theta}\rangle\langle\psi_{\theta}|]$, and I denotes the identity 2×2 matrix. Note that the parameters p and θ hold the following conditions of $p \in [0, 1]$, and $\theta \in [0, \frac{\pi}{4}]$, respectively. For simplicity, we define a parameter γ to determine the ratio between $|00\rangle$ and $|11\rangle$ as

$$\gamma = \frac{\cos^2 \theta}{\sin^2 \theta} = \cot^2 \theta. \quad (5)$$

The noise model of the state ρ can be described as follows. Alice prepares a bipartite entangled state of $|\psi\rangle_{\theta}$, and sends one of the particles to Bob while keeping the other. If the transmission channel has depolarizing noise with probability of $1-p$, the shared two-qubit state will become ρ as in Eq. (4).

Let us consider entanglement, Bell nonlocality and steerability of the state ρ . Here, we provide the results of the estimation with only brief explanation. Detailed estimation procedure can be found in Appendix.

Considering concurrence of the state ρ [33, 34], it is not difficult to find that ρ is entangled for $p > 1/3$. For investigating Bell nonlocality, we need to consider the correlation matrix Λ^{ρ} as

$$\Lambda_{ij}^{\rho} = \text{Tr}[\sigma_i \otimes \sigma_j \cdot \rho], \quad (6)$$

where $\{i, j\} \in \{x, y, z\}$ and σ_i s are Pauli matrices. The eigenvalues of $(\Lambda^{\rho})^T \cdot \Lambda^{\rho}$, where the superscript T denotes for transposition, are p^2 and $p^2 \sin^2 2\theta$ (with degeneracy). Hence, according to the Horodecki criterion [35], the state ρ is Bell nonlocal if

$$p > \frac{1}{\sqrt{1 + \sin^2 2\theta}}. \quad (7)$$

In order to check the steerability of ρ , we need to examine the steering inequality of Eq. (3). For simplicity, we choose $\mathcal{A}_1, \mathcal{B}_1 = \sigma_z$ and $\mathcal{A}_2, \mathcal{B}_2 = \sigma_x$. Note that the above observables are optimized for pure entangled states $|\psi_{\theta}\rangle$, so it can reveal all the steerable states [28]. Then, the left-hand side of Eq. (3) becomes $T = (2 + p + p \sin 2\theta)/4$ for ρ . Hence, the state ρ is steerable if

$$p > \frac{1}{1 + \sin 2\theta}. \quad (8)$$

In order to reveal hidden quantum correlation, we first examine the local filters of Alice and Bob as

$$\mathcal{F}_A = \begin{pmatrix} \frac{1}{\cos\theta} & 0 \\ 0 & \frac{1}{\sin\theta} \end{pmatrix}, \quad \mathcal{F}_B = \begin{pmatrix} 1 & 0 \\ 0 & 1 \end{pmatrix}. \quad (9)$$

After the local filters, the initial state ρ becomes a Werner state as

$$\rho_{\mathcal{F}} = \rho_{\pi/4} = p |\psi_{\frac{\pi}{4}}\rangle\langle\psi_{\frac{\pi}{4}}| + (1-p) \frac{I}{2} \otimes \frac{I}{2}. \quad (10)$$

The filtered state $\rho_{\mathcal{F}}$ is entangled for $p > 1/3$. The eigenvalues of $(\Lambda^{\rho_{\mathcal{F}}})^T \cdot \Lambda^{\rho_{\mathcal{F}}}$ are p^2 (with degeneracy), and

thus, $\rho_{\mathcal{F}}$ is Bell nonlocal for $p > 1/\sqrt{2}$. Therefore, the state ρ shows hidden Bell nonlocality with local filters of $\mathcal{F}_{A,B}$ for

$$\frac{1}{\sqrt{2}} < p \leq \frac{1}{\sqrt{1 + \sin^2 2\theta}}. \quad (11)$$

Since the final state $\rho_{\mathcal{F}}$ is a Werner state, it is steerable for $p > 1/2$ [3, 4, 28]. Therefore, local filters of Eq. (9) reveals hidden steerability for $1/2 < p \leq \frac{1}{1 + \sin 2\theta}$ of the state ρ . Note that for the region of $\frac{1}{2} < p < \frac{1}{\sqrt{2}}$, ρ shows hidden steerability but not Bell nonlocality. This result clearly shows that hidden steerability is distinct from hidden Bell nonlocality.

Now, let us consider another local filters of

$$\mathcal{G}_A = \begin{pmatrix} \frac{1}{\sqrt{\cos \theta}} & 0 \\ 0 & \frac{1}{\sqrt{\sin \theta}} \end{pmatrix}, \quad \mathcal{G}_B = \begin{pmatrix} \frac{1}{\sqrt{\sin \theta}} & 0 \\ 0 & \frac{1}{\sqrt{\cos \theta}} \end{pmatrix}. \quad (12)$$

The filtered state $\rho_{\mathcal{G}}$ is complicated, however, can be obtained by the state transformation of

$$\rho_{\mathcal{G}} = \frac{(\mathcal{G}_A \otimes \mathcal{G}_B) \cdot \rho \cdot (\mathcal{G}_A^\dagger \otimes \mathcal{G}_B^\dagger)}{\text{Tr}[(\mathcal{G}_A \otimes \mathcal{G}_B) \cdot \rho \cdot (\mathcal{G}_A^\dagger \otimes \mathcal{G}_B^\dagger)]}. \quad (13)$$

The filtered state $\rho_{\mathcal{G}}$ is entangled for $p > 1/3$. Based on the Horodecki criterion [35], the state $\rho_{\mathcal{G}}$ is Bell nonlocal for

$$(p^2 - 1) \csc \theta \sec \theta + 5p^2 + (p + 1)^2 \csc^2 2\theta - 2p + 1 > \frac{1}{2} [(p + 1) \csc \theta \sec \theta - 2p + 2]^2. \quad (14)$$

On the other hand, the steering parameter T of Eq. (3) of the state $\rho_{\mathcal{G}}$ is calculated as

$$T = \frac{(p + 1) \cot \theta}{2[(p + 1) \cot \theta - p + 1]} + \frac{(p + 1)(\tan \theta + \cot \theta + 2)}{4[(p + 1) \csc \theta \sec \theta - 2p + 2]}. \quad (15)$$

Thus, the state $\rho_{\mathcal{G}}$ is steerable for $p > \delta$, where

$$\delta = \left[\cot \theta - \cos^2 \theta (\cot \theta + 2) - 7 \sin \theta \cos \theta + \sin^2 \theta \sqrt{\csc^4 \theta (6 \sin 2\theta + 5 \sin 4\theta + 6 \cos 2\theta + 10)} \right] / \left[2(-2 \sin 2\theta + \cos 2\theta + 2) \right]. \quad (16)$$

Therefore, the state ρ shows hidden steerability for any value of p chosen from

$$\delta < p \leq \frac{1}{1 + \sin 2\theta}. \quad (17)$$

We summarize different regions of quantum correlation of the state ρ of Eq. (4) with respect to the parameters θ

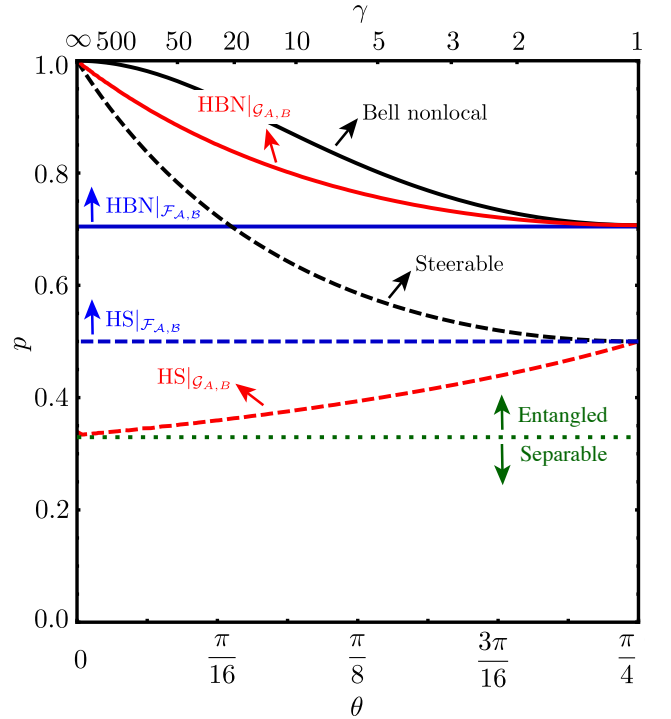


FIG. 1. The regions of various quantum correlation for a bipartite state ρ of Eq. (4) depending on the parameters p and θ . The boundaries of Bell nonlocality and quantum steerability are presented by solid and dashed lines, respectively. The steerability is determined by the fine-grained criterion with the observables of $A, B \in \{\sigma_z, \sigma_x\}$. Different colors denote for applying different local filters. $\text{HBN}|_{\mathcal{H}_{A,B}}$ and $\text{HS}|_{\mathcal{H}_{A,B}}$ denote hidden Bell nonlocal and hidden steerable with local filters of $\mathcal{H}_{A,B} \in \{\mathcal{F}_{A,B}, \mathcal{G}_{A,B}\}$, respectively.

and p in Fig. 1. It shows that, for $\theta = \pi/4$ or $\gamma = 1$, the states ρ become Werner states and they do not show any hidden quantum correlation. As θ decreases, both $\mathcal{F}_{A,B}$ and $\mathcal{G}_{A,B}$ become effective and the states reveal hidden quantum correlation.

Let us present the results of applying $\mathcal{F}_{A,B}$. As shown in Eq. (10), $\mathcal{F}_{A,B}$ make the initial state ρ which has biased $\gamma > 1$ to a Werner state $\rho_{\pi/4}$ or equivalently $\gamma = 1$ while keeping the parameter p unchanged. Therefore, $\mathcal{F}_{A,B}$ uncover hidden Bell nonlocality and steerability of ρ up to those of the Werner state $\rho_{\pi/4}$. In Fig. 1, these are represented as horizontal straight lines.

The results of applying $\mathcal{G}_{A,B}$ are more interesting. Comparing to $\mathcal{F}_{A,B}$, the region for hidden Bell nonlocality is decreased. However, the region for hidden steerability is enlarged comparing to the $\mathcal{F}_{A,B}$ case. Therefore, if we determine the effectiveness of local filters as the area of uncovered nonlocal correlation region, $\mathcal{G}_{A,B}$ are less effective on revealing Bell nonlocality than $\mathcal{F}_{A,B}$. On the other hand, $\mathcal{G}_{A,B}$ are more effective on uncovering steerability than $\mathcal{F}_{A,B}$. These results intimate the structural different between Bell nonlocality and steering.

It is remarkable that as $\theta \rightarrow 0$ (or equivalently, $\gamma \rightarrow$

∞), the region of hidden steerability revealed by $\mathcal{G}_{A,B}$ is broadened while the regions of other quantum correlation contracted or remain the same. Note that the amount of entanglement decreases as $\theta \rightarrow 0$ for a fixed p . Therefore, it suggests a counter-intuitive result that mixed states from non-maximally pure entangled states can have hidden steerability for more wide range of a mixing parameter than the mixed state originated from a maximally pure entangled state.

III. EXPERIMENT

Figure 2 shows the experimental setup to explore hidden quantum correlation. First, let us describe the initial state preparation as shown in Fig. 2 (a). Maximally polarization entangled photon pairs of $|\psi\rangle = \frac{1}{\sqrt{2}}(|00\rangle + |11\rangle) = \frac{1}{\sqrt{2}}(|HH\rangle + |VV\rangle)$ centered at 780 nm are generated at a sandwich BBO crystal via the SPDC process pumped by a femtosecond pump pulse centered at 390 nm. Here, $|H\rangle$ and $|V\rangle$ denote horizontal and vertical polarization states, respectively. The sandwich BBO crystal, which is composed of two type-II BBO crystals and a half waveplate, is specially designed for efficient generation of two-photon entangled states [36]. Each of the entangled photon pairs is then sent to Alice and Bob, respectively.

The parameter θ or equivalently γ is controlled by partially polarizing beamsplitters (PPBS) at Alice. The transmittivity of horizontal and vertical polarization states of the PPBS are $T_H = 1$ and $T_V = \frac{1}{3}$, respectively. The depolarizing channel can be implemented by statistically mixing identity (I) and three Pauli operations ($\sigma_x, \sigma_y, \sigma_z$) with a set of waveplates (QHQ) placed at Bob [37–39]. The noise parameter p is determined by adjusting the ratio of the single-qubit operations during the data acquisition.

Since we use the single-photon polarization qubits, the local filters $\mathcal{F}_{1,2}$ and $\mathcal{G}_{1,2}$ correspond to polarization dependent loss [40]. As depicted in Fig. 2(b), the local filtering operations are implemented by a set of beam displacers (BD) and half waveplates (HWP) for high phase

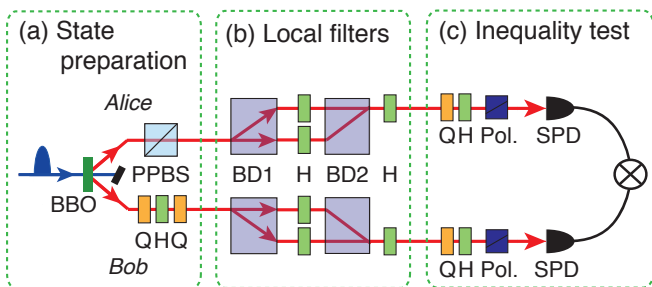


FIG. 2. Experimental setup. PPBS: partially polarizing beamsplitter, Q: quarter waveplate, H: half waveplate, BD: beam displacer, Pol.: polarizer, SPD: single-photon detector. See text for details.

stability [41]. While the vertically polarized beam is transmitted through the BD1, the horizontal polarization state is displaced after the BD1. Then, the polarization state at each arm is flipped by the following HWP at 45° , and two beams are combined together at BD2. The amount of the polarization dependent loss can be adjusted by changing the angles of HWPs between two BDs. In order to restore the flipped polarization state, we put a HWP at 45° after the second BD.

The experimental tests of Bell's and steering inequalities require various two-qubit projection measurements, which can be implemented by waveplates, polarizers, and single-photon detectors as shown in Fig. 2(c). The coincidence detection between Alice and Bob is achieved by a home-made coincidence counting unit [42].

In order to obtain maximal Bell parameter S , Alice and Bob should choose different observables for different shared states [43–45]. In particular, for the states ρ , Alice and Bob choose their observables of $\mathcal{A} \in \{\sigma_z, \sigma_x\}$, and $\mathcal{B} \in \{\sigma_z \cos \varphi_1 + \sigma_x \sin \varphi_1, \sigma_z \cos \varphi_2 + \sigma_x \sin \varphi_2\}$ where $\varphi_1 = \pi + \arctan \left[\frac{\sqrt{4\gamma/(1+\gamma)^2}}{\sqrt{\frac{1}{\gamma}(\gamma+1)(p+1)+2(p-1)}} \right]$ and $\varphi_2 = \arctan \left[-\frac{\sqrt{4\gamma/(1+\gamma)^2}}{\sqrt{\frac{1}{\gamma}(\gamma+1)(p+1)+2(p-1)}} \right]$, respectively. For Werner states $\rho_{\mathcal{F}}$, Alice's and Bob's observables are $\mathcal{A} \in \{\sigma_z, \sigma_x\}$ and $\mathcal{B} \in \{-(\sigma_z + \sigma_x)/\sqrt{2}, (\sigma_z - \sigma_x)/\sqrt{2}\}$. For the case of $\rho_{\mathcal{G}}$, $\mathcal{A} \in \{\sigma_z, \sigma_x\}$, and $\mathcal{B} \in \{\sigma_z \cos \varphi_1 + \sigma_x \sin \varphi_1, \sigma_z \cos \varphi_2 + \sigma_x \sin \varphi_2\}$ where $\varphi_1 = \pi + \arctan \left[\frac{4p}{\sqrt{\frac{1}{\gamma}(\gamma+1)(p+1)+2(p-1)}} \right]$ and $\varphi_2 = \arctan \left[-\frac{4p}{\sqrt{\frac{1}{\gamma}(\gamma+1)(p+1)+2(p-1)}} \right]$, respectively.

We present the theoretical and experimental Bell parameter S with respect to the parameter p for $\gamma = 1$ and 9 in Fig. 3(a). Note that theoretical values for ρ with $\gamma = 1$ and $\rho_{\mathcal{F}}$ with $\gamma = 9$ are the same since both states are Werner states. For $\gamma = 1$, we only present the results for ρ since both local filters $\mathcal{F}_{A,B}$ and $\mathcal{G}_{A,B}$ become identity. Both theoretical and experimental results show that the Bell parameter S decreases as noise increases or equivalently p decreases. For $\gamma = 9$, we can see that though both filters of $\mathcal{F}_{A,B}$ and $\mathcal{G}_{A,B}$ can reveal hidden Bell nonlocality, $\mathcal{F}_{A,B}$ are more effective than $\mathcal{G}_{A,B}$ to uncover Bell nonlocality. For example, $\mathcal{G}_{A,B}$ fails to uncover hidden Bell nonlocality for $p = 0.8$ while $\mathcal{F}_{A,B}$ successfully find it. It is noteworthy to remark that the region of hidden Bell nonlocality can be as large as that of the state ρ with $\gamma = 1$ (i.e., mixed states originated from maximally pure entangled state) with the local filters $\mathcal{F}_{A,B}$, and never exceed this limit. This means that the hidden Bell nonlocality boundaries of mixed states from non-maximally pure entangled states can be stretched to the Bell nonlocality boundary of the mixed state from maximally pure entangled states.

The steering inequality of Eq. (3) is tested with the observables of $\mathcal{A}, \mathcal{B} \in \{\sigma_z, \sigma_x\}$. In particular, the steering parameter T is experimentally obtained by the equation

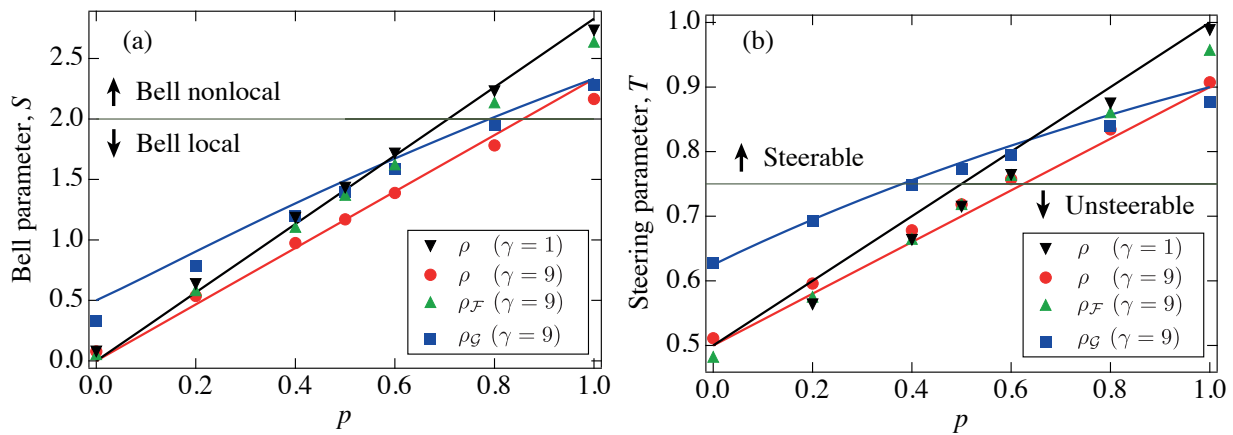


FIG. 3. Theoretical and experimental results of (a) Bell nonlocality and (b) steerability for $\gamma = 1$ and 9. Since local filters of $\mathcal{F}_{A,B}$ and $\mathcal{G}_{A,B}$ become identity operation, we only present ρ for $\gamma = 1$ case. Black line corresponds to the theoretical values of Werner states, i.e., ρ with $\gamma = 1$ and $\rho_{\mathcal{F}}$ with $\gamma = 9$. Red and blue lines are the theoretical values for the states ρ , and $\rho_{\mathcal{G}}$ with $\gamma = 9$, respectively. Error bars are smaller than the size of markers.

given as,

$$T = \frac{1}{2} \left(\frac{N_{HH}}{N_{HH} + N_{HV}} + \frac{N_{DD}}{N_{DD} + N_{DA}} \right), \quad (18)$$

where N_{XY} denotes the coincidence counts of X and Y projection measurements on Alice and Bob, respectively. The subscripts H, V, D , and A are horizontal, vertical, diagonal, and anti-diagonal polarization states, respectively.

Figure 3(b) presents the theoretically and experimentally obtained steering parameter T with respect to the parameter p of the states ρ , $\rho_{\mathcal{F}}$ and $\rho_{\mathcal{G}}$ for $\gamma = 1$ and 9. Similarly to the Bell nonlocality result, the theoretical values of ρ for $\gamma = 1$ are identical to those of $\rho_{\mathcal{F}}$ with $\gamma = 9$. It shows that while both $\mathcal{F}_{A,B}$ and $\mathcal{G}_{A,B}$ can reveal hidden steerability, $\mathcal{G}_{A,B}$ are more effective than $\mathcal{F}_{A,B}$ for uncovering hidden steerability. In particular, $\mathcal{G}_{A,B}$ successfully uncover hidden steerability for $p = 0.5$ while $\mathcal{F}_{A,B}$ fails. In addition, we note that the states with $p = 0.6$ and 0.5 show hidden steerability while they fail to show hidden Bell nonlocality. These results clearly show that the region for hidden steerability is more wide than that of hidden Bell nonlocality.

It is interesting to compare the results of ρ with $\gamma = 1$ and $\rho_{\mathcal{G}}$ with $\gamma = 9$. Both theoretical and experimental results clearly shows the steerability boundary of $\rho_{\mathcal{G}}$ with $\gamma = 9$ can reach smaller p , meaning more noise, than that of ρ with $\gamma = 1$. In particular, for $p = 0.5$, $\rho_{\mathcal{G}}$ with $\gamma = 9$ states successfully reveal steerability whereas ρ with $\gamma = 1$ fails. This experimental result supports our theoretical finding that mixed states from non-maximally

pure entangled states can have hidden steerability for more wide range of the noise parameter than the mixed state originated from a maximally pure entangled state.

IV. CONCLUSION

In conclusion, we have theoretically and experimentally investigated revealing of hidden steerability with local filtering operations. We have proven that hidden steerability is distinguishable from hidden Bell nonlocality by showing that there are quantum states which reveal hidden steerability, but fail to show hidden Bell nonlocality. We have investigated two sets of local filters and found that one filter set is more effective on revealing hidden Bell nonlocality whereas the other is more effective on uncovering hidden steerability. We have also presented a counter-intuitive result that mixed states from non-maximally pure entangled states can have hidden steerability even when the mixed state originated from a maximally pure entangled state does not have steerability. Considering the fundamental importance and applications of quantum steerability in quantum information science, our findings provide a better understanding of nonlocal quantum correlation and paves the way towards secure quantum communications.

ACKNOWLEDGEMENT

This work was supported by the ICT R&D program of MSIP/IITP (B0101-16-1355), and the KIST research programs (2E27231, 2V05340).

[1] A. Einstein, D. Podolsky, and N. Rosen, Phys. Rev. **47**, 777 (1935).

[2] J. S. Bell, Physics **1**, 195 (1964)

- [3] H. M. Wiseman, S. J. Jones, and A. C. Doherty, *Phys. Rev. Lett.* **98**, 140402 (2007).
- [4] S. J. Jones, H. M. Wiseman, and A. C. Doherty, *Phys. Rev. A* **76**, 052116 (2007).
- [5] N. Brunner, D. Cavalcanti, S. Pironio, V. Scarani, and S. Wehner, *Rev. Mod. Phys.* **86**, 419 (2014).
- [6] E. Schrödinger, *Proc. Cambridge Philos. Soc.* **31**, 553 (1935).
- [7] D. J. Saunders, S. J. Jones, H. M. Wiseman, and G. J. Pryde, *Nature Phys.* **6**, 845 (2010).
- [8] C. Branciard, E. G. Cavalcanti, S. P. Walborn, V. Scarani, and H. M. Wiseman, *Phys. Rev. A* **85**, 010301(R) (2012).
- [9] J. Barrett, L. Hardy, and A. Kent, *Phys. Rev. Lett.* **95**, 010503 (2005).
- [10] A. Acín, N. Brunner, N. Gisin, S. Massar, S. Pironio, and V. Scarani, *Phys. Rev. Lett.* **98** 230501 (2007).
- [11] U. Vazirani, and T. Vidick, *Phys. Rev. Lett.* **113**, 140501 (2014).
- [12] E. A. Aguilar, R. Ramanathan, J. Kofler, and M. Pawłowski, *Phys. Rev. A* **94**, 022305 (2016).
- [13] A. J. Bennet, D. A. Evans, D. J. Saunders, C. Branciard, E. G. Cavalcanti, H. M. Wiseman, and G. J. Pryde, *Phys. Rev. X* **2**, 031003 (2012).
- [14] B. Wittmann, S. Ramelow, F. Steinlechner, N. K. Langford, N. Brunner, H. Wiseman, R. Ursin, and A. Zeilinger, *New J. Phys.* **14**, 053030 (2012).
- [15] D. H. Smith, G. Gillett, M. P. de Almeida, C. Branciard, A. Fedrizzi, T. J. Weinhold, A. Lita, B. Calkins, T. Gerrits, H. M. Wiseman, S. W. Nam, and A. G. White, *Nature Comm.* **3**, 625 (2012).
- [16] C.-Y. Hsieh, Y.-C. Liang, and R.-K. Lee, *Phys. Rev. A* **94**, 062120 (2016).
- [17] Y.-C. Liang, and A. Doherty, *Phys. Rev. A* **73**, 052116 (2006).
- [18] M. Navascúes, and T. Vértesi, *Phys. Rev. Lett.* **106**, 060403 (2011).
- [19] C. Palazuelos, *Phys. Rev. Lett.* **109**, 190401 (2012).
- [20] S. Popescu, *Phys. Rev. Lett.* **74**, 2619 (1995).
- [21] N. Gisin, *Phys. Lett. A* **210**, 151 (1996).
- [22] P. G. Kwiat, S. Barraza-Lopez, A. Stefanov, and N. Gisin, *Nature* **409**, 1014 (2001).
- [23] F. Verstraete, and M. M. Wolf, *Phys. Rev. Lett.* **89**, 170401 (2002).
- [24] L. Masanes, *Phys. Rev. Lett.* **100**, 090403 (2008).
- [25] Y.-C. Liang, L. Masanes, and D. Rosset, *Phys. Rev. A* **86**, 052115 (2012).
- [26] S. P. Walborn, A. Salles, R. M. Gomes, F. Toscano, and P. H. Souto Ribeiro, *Phys. Rev. Lett.* **106**, 130402 (2011).
- [27] J. Schneeloch, C. J. Broadbent, S. P. Walborn, E. G. Cavalcanti, and J. C. Howell, *Phys. Rev. A* **87**, 062103 (2013).
- [28] T. Pramanik, M. Kaplan, and A. S. Majumdar, *Phys. Rev. A* **90**, 050305(R) (2014).
- [29] P. Skrzypczyk, M. Navascúes, and D. Cavalcanti, *Phys. Rev. Lett.* **112**, 180404 (2014).
- [30] P. Chowdhury, T. Pramanik, and A. S. Majumdar, *Phys. Rev. A* **92**, 042317 (2015).
- [31] I. Kogias, A. R. Lee, S. Ragy, and G. Adesso, *Phys. Rev. Lett.* **114**, 060403 (2015).
- [32] J. Bowles, F. Hirsch, M. Túlio Quintino, and N. Brunner, *Phys. Rev. A* **93**, 022121 (2016).
- [33] S. Hill and W. K. Wootters, *Phys. Rev. Lett.* **78**, 5022(1997).
- [34] W. K. Wootters, *Phys. Rev. Lett.* **80**, 2245 (1998).
- [35] R. Horodecki, P. Horodecki and M. Horodecki, *Phys. Lett. A* **200**, 340 (1995).
- [36] X.-L. Wang, L.-K. Chen, W. Li, H.-L. Huang, C. Liu, C. Chen, Y.-H. Luo, Z.-E. Su, D. Wu, Z.-D. Li, H. Lu, Y. Hu, X. Jiang, C.-Z. Peng, L. Li, N.-L. Liu, Y.-A. Chen, C.-Y. Lu, and J.-W. Pan, *Phys. Rev. Lett.* **117**, 210502 (2016).
- [37] H.-T. Lim, Y.-S. Ra, Y.-S. Kim, J. Bae, and Y.-H. Kim, *Phys. Rev. A* **83**, 020301(R), (2011).
- [38] H.-T. Lim, Y.-S. Kim, Y.-S. Ra, J. Bae, and Y.-H. Kim, *Phys. Rev. Lett.* **107**, 160401, (2011).
- [39] H.-T. Lim, Y.-S. Kim, Y.-S. Ra, J. Bae, and Y.-H. Kim, *Phys. Rev. A* **86**, 042334, (2012).
- [40] Y.-S. Kim, Y.-W. Cho, Y.-S. Ra, and Y.-H. Kim, *Opt. Express* **17**, 11978 (2009).
- [41] Y.-S. Kim, O. Kwon, S. M. Lee, J.-C. Lee, H. Kim, S.-K. Choi, H. S. Park, and Y.-H. Kim, *Opt. Express* **19**, 24957 (2011).
- [42] B.-K. Park, Y.-S. Kim, O. Kwon, S.-W. Han, and Y.-H. Kim, *Appl. Opt.* **54** 4727 (2015).
- [43] N. Gisin, *Phys. Lett. A* **154**, 201-202 (1991).
- [44] N. Gisin, and A. Peres, *Phys. Lett. A* **162**, 15 (1992).
- [45] S. Popescu, and D. Rohrlich, *Phys. Lett. A* **166**, 293 (1992).

Appendix A: Calculation of entanglement

To measure the entanglement of a bipartite state, we calculate concurrence of the state. If concurrence is positive, then the state is entangled. The concurrence of the state ρ can be calculated from the eigenvalues of $\Lambda^C = \rho \cdot (\sigma_y \otimes \sigma_y \cdot \rho^* \cdot \sigma_y \otimes \sigma_y)$ where the asterisk '*' stands for complex conjugation. For the state ρ , the eigenvalues of Λ^C in decreasing order becomes

$$\begin{aligned}\lambda_1 &= \frac{1}{16}(3p+1)^2 \sin^2 2\theta, \\ \lambda_2 = \lambda_3 = \lambda_4 &= \frac{1}{16}(1-p)^2 \sin^2 2\theta.\end{aligned}\tag{A1}$$

The concurrence of the state ρ is

$$\begin{aligned}C^\rho &= \max \left[\sqrt{\lambda_1} - \sqrt{\lambda_2} - \sqrt{\lambda_3} - \sqrt{\lambda_4}, 0 \right] \\ &= \max \left[(3p-1) \sin \theta \cos \theta, 0 \right].\end{aligned}\tag{A2}$$

For the Werner states $\rho_{\mathcal{F}}$, $C^{\rho_{\mathcal{F}}} = \frac{3p-1}{2}$ since $\theta = \frac{\pi}{4}$.

Similarly, one can calculate concurrence of the state $\rho_{\mathcal{G}}$. The eigenvalues of Λ^C in decreasing order are

$$\begin{aligned}\lambda_1 &= \left[\frac{3p+1}{(p+1) \csc \theta \sec \theta - 2p+2} \right]^2, \\ \lambda_2 = \lambda_3 = \lambda_4 &= \frac{1-p}{(p+1) \csc \theta \sec \theta - 2p+2}.\end{aligned}\tag{A3}$$

Therefore, concurrence of the state $\rho_{\mathcal{G}}$ is

$$C^{\rho_{\mathcal{G}}} = \max \left[\frac{6p-2}{(p+1) \csc \theta \sec \theta - 2p+2}, 0 \right].\tag{A4}$$

Appendix B: Calculation of measurement settings for Bell nonlocality

To obtain maximum Bell violation for the bipartite state ρ , Alice measures either observables $\mathcal{A}_1 = \sigma_x$ or $\mathcal{A}_2 = \sigma_z$ on her system A . Bob's choice of observables are

$$\begin{aligned}\mathcal{B}_1 &= \sigma_z \cos \varphi_1 + \sigma_x \sin \varphi_1, \\ \mathcal{B}_2 &= \sigma_z \cos \varphi_2 + \sigma_x \sin \varphi_2.\end{aligned}\tag{B1}$$

The value of Bell parameter S becomes

$$\begin{aligned}S^\rho &= \text{Tr} [\mathcal{A}_1 \mathcal{B}_1 + \mathcal{A}_1 \mathcal{B}_2 + \mathcal{A}_2 \mathcal{B}_1 - \mathcal{A}_2 \mathcal{B}_2] \\ &= p [\sin 2\theta (\sin \varphi_1 + \sin \varphi_2) + \cos \varphi_1 - \cos \varphi_2].\end{aligned}\tag{B2}$$

The maximum value of S^ρ can be found when $\cos \varphi_1 = -\cos \varphi_2 = \frac{1}{\sqrt{1+\sin^2 2\theta}}$, $\sin \varphi_1 > 0$, and $\sin \varphi_2 > 0$. Therefore, Bob's measurement settings corresponding to the maximum value of Bell parameter S^ρ are

$$\begin{aligned}\varphi_1 &= \pi + \arctan [\sin^2 2\theta] = \pi + \arctan \left[\sqrt{4\gamma/(1+\gamma)^2} \right] \\ \varphi_2 &= \arctan [-\sin^2 2\theta] = \arctan \left[-\sqrt{4\gamma/(1+\gamma)^2} \right].\end{aligned}\tag{B3}$$

In the case of Werner state $\rho_{\mathcal{F}}$, or equivalently $\theta = \frac{\pi}{4}$, Bob's choice of measurement settings become $\mathcal{B}_1 = \sigma_x$ and $\mathcal{B}_2 = \sigma_z$, respectively.

The value of Bell parameter S for the state $\rho_{\mathcal{G}}$ with the set of Alice's Bob's observables $\{\mathcal{A}_1 = \sigma_x, \mathcal{A}_2 = \sigma_z\}$, and $\mathcal{B}_{1,2}$ given by Eq. (B1) becomes

$$S^{\rho_{\mathcal{G}}} = \frac{8 \left((p^2-1) \csc \theta \sec \theta + (p+1)^2 \csc^2 2\theta + p(5p-2) + 1 \right)}{(4(p+1)^2 \csc^2 2\theta - 4(p-1)^2) \sqrt{\frac{16p^2}{((p+1) \csc \theta \sec \theta + 2(p-1))^2} + 1}}.\tag{B4}$$

It is not difficult to obtain the Bob's observables corresponding to maximum value of the Bell parameter S^{ρ_G} as

$$\begin{aligned}\varphi_1 &= \pi + \arctan\left(\frac{4p}{(p+1)\csc\theta\sec\theta + 2(p-1)}\right) = \pi + \arctan\left[\frac{4p}{\sqrt{\frac{1}{\gamma}(\gamma+1)(p+1) + 2(p-1)}}\right], \\ \varphi_2 &= \arctan\left(-\frac{4p}{(p+1)\csc\theta\sec\theta + 2(p-1)}\right) = \arctan\left[-\frac{4p}{\sqrt{\frac{1}{\gamma}(\gamma+1)(p+1) + 2(p-1)}}\right].\end{aligned}\quad (\text{B5})$$

Appendix C: Calculation of steerability

For the observables of $\mathcal{A}, \mathcal{B} \in \{\sigma_z, \sigma_x\}$, the conditional probability distribution $P(b = 0_{\mathcal{B}}|a = 0_{\mathcal{A}})$ for the shared state ρ becomes

$$\begin{aligned}P(0_{\sigma_z}|0_{\sigma_z}) &= \frac{1+p}{2}, \\ P(0_{\sigma_x}|0_{\sigma_x}) &= \frac{1+p\sin 2\theta}{2}.\end{aligned}\quad (\text{C1})$$

Therefore, the steering parameter T given by Eq.(3) for the outcomes $a = b = 0$ becomes

$$\begin{aligned}T^\rho &= \frac{1}{2} \sum_{i=z,x} P(b = 0_{\sigma_i}|a = 0_{\sigma_i}) \\ &= \frac{2+p+p\sin 2\theta}{4}.\end{aligned}\quad (\text{C2})$$

The value of the steering parameter T for Werner state $\rho_{\mathcal{F}}$ can be obtain from Eq. (C2) for the choice $\theta = \pi/4$, and it becomes

$$T^{\rho_{\mathcal{F}}} = \frac{1+p}{2}.\quad (\text{C3})$$

Similarly, the conditional probability distribution $P(b = 0_{\mathcal{B}}|a = 0_{\mathcal{A}})$ for the shared state ρ_G becomes

$$\begin{aligned}P(0_{\sigma_z}|0_{\sigma_z}) &= \frac{(p+1)\cot\theta}{(p+1)\cot\theta - p + 1}, \\ P(0_{\sigma_x}|0_{\sigma_x}) &= \frac{2p}{(p+1)\csc\theta\sec\theta - 2p + 2}.\end{aligned}\quad (\text{C4})$$

Therefore, the steering parameter T of the state ρ_G for the outcomes $a = b = 0$ becomes

$$\begin{aligned}T^{\rho_G} &= \frac{1}{2} \sum_{i=z,x} P(b = 0_{\sigma_i}|a = 0_{\sigma_i}) \\ &= \frac{1}{2 - \frac{2(p-1)\tan\theta}{p+1}} + \frac{p}{(p+1)\csc\theta\sec\theta - 2p + 2}.\end{aligned}\quad (\text{C5})$$